



## Clarification of a laterite suspension using a mixed two-layer filter based on limestone and pozzolan

Nguemtue Nguemtue Thierry<sup>1,2</sup>, Nsoe Mengue Jean Jacques Nestor<sup>1,2\*</sup>, Amba Esegni Victoria<sup>2</sup>, Nouria Zihane<sup>2</sup>, Kofa Guillaume Patrice<sup>2</sup>, Ndi Koungou Sylvere<sup>2</sup>, Kayem Guifo Joseph<sup>2</sup>.

<sup>1</sup>Laboratory of Chemical Engineering and Environment, University Institute of Technology (IUT), University of Ngaoundere, P.O. Box 455, Ngaoundere, Cameroon.

<sup>2</sup>Water Treatment and Filtration Research (Chem. Eng.) Group, Department of Process Engineering, ENSAI, University of Ngaoundere, P.O. Box 455, Ngaoundere, Cameroon.

\*Corresponding author: [nsoemenguenestor@yahoo.fr](mailto:nsoemenguenestor@yahoo.fr)

### Key words

### Abstract

Clarification,  
Laterite suspension,  
Mixed/coat filter,  
Limestone/pozzolan.

Coagulation and flocculation are essential in water clarification but rely on costly chemical reagents that can leave harmful residues and generate polluting sludge. This study aims to evaluate and compare the effectiveness of bilayer (limestone/pozzolan) and mixed (homogeneous blend) filters for clarifying lateritic suspensions. A suspension with  $30 \pm 1$  NTU turbidity and  $\text{pH } 6.00 \pm 0.05$  was prepared. Filters were composed of pozzolan and limestone granules (1–2 mm) and characterized by porosity, permeability, bed surface area, and Reynolds number. Flow behavior was determined using a 1 M glucose solution. The bilayer and mixed filters showed porosities of 67.24% and 62.49%, permeabilities of  $3.51 \times 10^{-7}$  and  $5.73 \times 10^{-7} \text{ m}^2$ , and bed surface areas of 2911.99 and 3334.22  $\text{m}^2$ , respectively. Reynolds numbers were 1.42 and 1.75, indicating piston flow in both systems. The mixed filter achieved 65% turbidity removal, outperforming the bilayer filter's 50%, and had a lower pressure drop (780 Pa vs. 820 Pa). These results suggest that the mixed filter offers better performance and efficiency, making it a promising alternative for the clarification of lateritic suspensions.

Received: 16.01.2025

Accepted: 17.04.2025

Published online: 06.05.2025

How to cite this article: Nguemtue, N. T., Nsoe Mengue, J. J. N., Amba Esegni, V., Nouria, Z., Kofa, G. P., Ndi Koungou, S., & Kayem Guifo, J. (2025). *Clarification of a laterite suspension using a mixed two-layer filter based on limestone and pozzolan*. *MJ Engineering Sciences*.1(1), 19-31. <https://doi.org/10.63156/mjes02>.

## 1. Introduction

The Adamaoua region of Cameroon is characterized by a geography rich in natural resources, particularly surface water bodies such as rivers and lakes (Tangwa et al., 2019; Raouf et al., 2025; Kepdieu et al., 2025; Chegaing et al., 2024). These surface waters are a primary source of water for local populations; however, they are frequently contaminated with suspended solids, mainly mineral particles such as clay and sand (Kameni et al., 2019). The concentration of these suspended particles increases significantly during the rainy season, when surface runoff leads to the presence of lateritic suspensions. These suspensions originate from soil erosion and consist of fine, colloidal particles (Lengay et al., 2019; Aguiza et al., 2014).

The presence of such colloidal matter poses challenges for both domestic water use and drinking water treatment, primarily due to the significant increase in turbidity, which affects the organoleptic properties of water (Moye et al., 2025; Abdou et al., 2024; Singh, 2024). Addressing this issue typically involves a multi-step treatment process comprising coagulation-flocculation, sedimentation, and granular filtration. However, the chemical reagents used during coagulation and flocculation may leave residual pollutants in the treated water (Kameni et al., 2019).

Granular filtration, an alternative or complementary method, operates by retaining pollutants as water flows through porous filter media (Legube, 2021). These media can consist of one or multiple layers of materials designed to trap suspended particles. Among the preferred materials for granular filtration is pozzolan, valued for its adsorption capacity and filtration efficiency (Wamba et al., 2017; Ndi et al., 2010; Ndi et al., 2008). Additionally, calcium carbonate ( $\text{CaCO}_3$ ) is sometimes incorporated due to its coagulating properties, capacity to mineralize water, and ability to neutralize acidity (Nguemtue et al., 2023; Nguemtue et al., 2020).

Granular filtration systems can be configured as monolayer, bilayer, or multilayer filters, each offering different advantages depending on local conditions. These configurations have been shown to be effective in treating turbid water. For instance, BesBes (2020) utilized both monolayer and bilayer setups for water clarification, while Basman et al. (2015) employed a bilayer configuration to reduce turbidity in oil-contaminated effluents following coagulation. Similarly, Badalians et al. (2012) and Villabona-Ortíz et al. (2022) explored various combinations of pozzolan and limestone in mono-, bi-, and multilayer filter systems with upstream coagulation treatment.

Despite these advances, no studies to date have specifically investigated the performance of mixed-material filter configurations for the removal of colloidal particles. Therefore, the overarching objective of this study is to evaluate and compare the effectiveness of bilayer and mixed-material filtration systems in clarifying lateritic suspensions.

## 2. Materials and Methods

### 2.1. Filter materials (limestone and pozzolan)

The samples of pozzolan used in this study came from the Djoungo quarry in the Littoral region of Cameroon. This site was chosen based on the work by Ndi et al., 2010, which demonstrated the adsorption and retention properties of micro-organisms by this pozzolan, geolocated at 4°35'N and 9°37'E. The limestone was sourced from the Bidzar quarry in the North region of Cameroon (Nguemtue et al., 2023), located at N 9°55'33", E 14°7'37.2".

### 2.2. Laterite

The laterite used was collected approximately 0.5 m from the surface of the earth to remove organic matter, mainly plant debris. Its geolocation is N 7°41'92"54; E 13°54'21"57.

### 2.3. Experimental set-up

The experimental set-up used for the laboratory tests consists of a 20-litre tank containing the well water sample. This water is fed into the 49.7 cm Plexiglas column with an internal diameter of 3.3 cm using a peristaltic pump, through a 187 cm-long pipe with a diameter of 0.2 cm. The upper part of the column has an overflow to maintain a

constant solution height (constant pressure) above the bed. At the bottom, a control valve is fitted to regulate the flow of water.

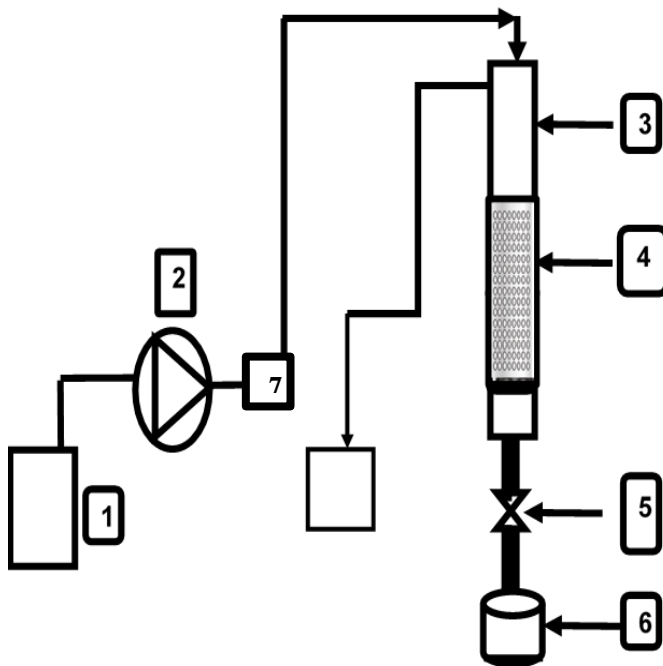


**Figure1:** Schematic diagram of the experimental column filtration system (1-synthetic effluent storage tank, 2-peristaltic pump, 3-plexiglass column, 4-filter media zone, 5-control valve, 6-filtrate storage tank, 7-overflow tank).

#### 2.4. Preparation of filter materials

Pozzolan and limestone were prepared following modified protocols adapted from Nguemtue et al. (2023) and Ndi et al. (2010). The preparation procedure involved crushing the raw materials and sieving them using standard 1 mm and 2 mm meshes to obtain particle sizes ranging from 1 to 2 mm. To ensure the cleanliness of the filter media, both pozzolan and limestone were repeatedly rinsed with distilled water until the conductivity of the supernatant matched that of the original distilled water. The materials were then dried in a MEMMERT oven at 105 °C for 8 hours, cooled to room temperature, and stored in sealed jars for further use. The main steps for obtaining pozzolan and limestone aggregates are illustrated in the following diagram.

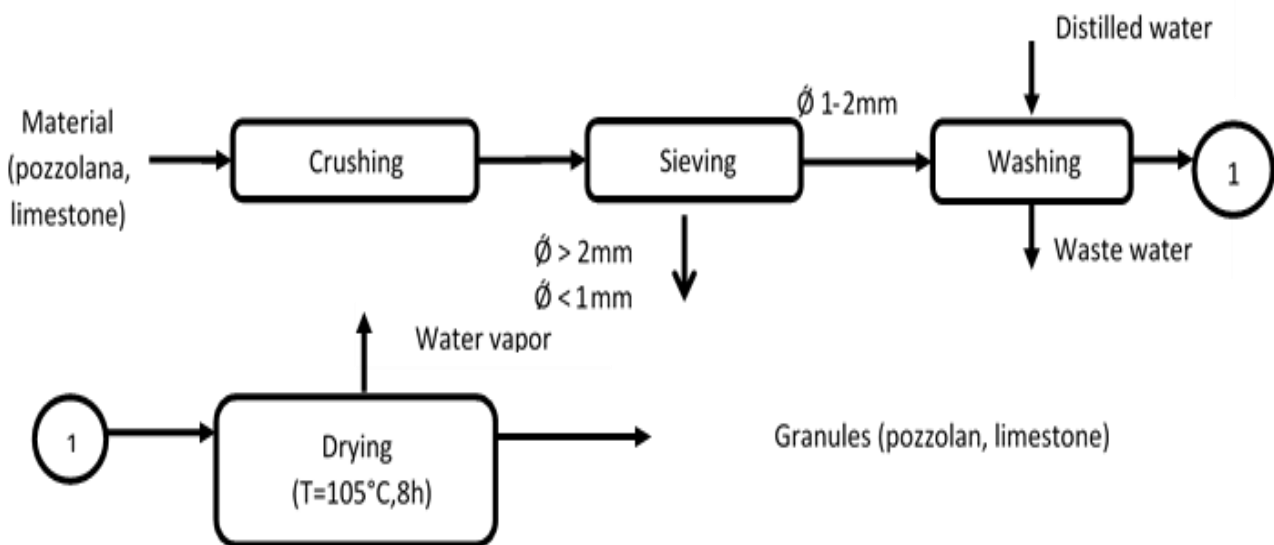


**Figure 2:** Schematic diagram for obtaining granules of the materials (pozzolan and limestone) (Ndi et al.,2010)

Distilled water was used to prepare the laterite suspension. The method used for this preparation is based on the Kameni et al., 2019 method. It consists of gradually purifying the laterite sample to rid it completely of organic matter. The laterite suspension obtained is stirred for homogenization using a KIKA Werke mechanical stirrer for two minutes. The supernatant was then collected and diluted with distilled water. The pH was adjusted with a NaOH solution. It was measured using a portable pH meter (Kedida CT-6021A) with built-in probes and adjusted with slaked lime or sulfuric acid. The pH obtained was  $6 \pm 0.05$ . To determine the turbidity of the laterite suspension, three beakers were successively filled with equal volumes (50 ml) of the previously obtained laterite suspension and then read with a Hach turbidimeter. The turbidity of the laterite suspension obtained was  $30 \text{ NTU} \pm 1$ . The temperature of the suspension was  $23^\circ\text{C} \pm 2$ .

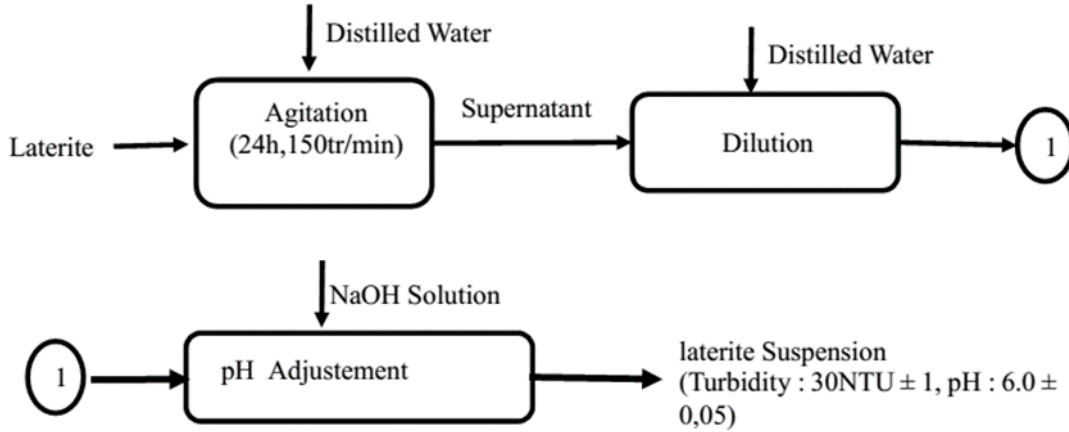


**Figure 3:** Schematic diagram of the preparation of the laterite suspension, modified from Kameni et al.,2019

In order to adjust the calcium ion concentration of the suspension,  $\text{CaCl}_2$  from RIDEL-DE HAËN AG was used (molar mass =  $110.99 \text{ g}\cdot\text{mol}^{-1}$ ; purity = 92.5%).

## 2.5. Hydrodynamic characterisation of the various fixed beds

A predetermined mass of pozzolan ( $169,93 \pm 0,04 \text{ g}$ ) is introduced into the column. Distilled water is then added up to the point of flush so as to saturate the pozzolan and/or limestone bed. The volume of water introduced represents the space not occupied by the pozzolan and/or limestone particles (the voids)  $V_V$ . The total volume of the bed ( $V_T$ ) is equal to the volume of the column over the height ( $H$ ) occupied by the pozzolan and/or limestone. It is determined by the usual formula for the volume of a cylinder.

$$V_T = \frac{\pi D^2}{4} H. \quad (1)$$

Where,  $D$  is the internal diameter of the column and  $H$  is the height of the bed.

these two volumes were used to calculate the porosity of bed ( $\epsilon$ ) following the equation 2

$$\epsilon = \frac{V_V}{V_T} = 1 - \frac{V_P}{V_t} \quad (2)$$

With  $V_p$ , the volume of the bed attributable to the adsorbent particles.

To determine the pressure drop ( $\Delta P/H$ ) per unit height, distilled water was passed at a given speed through the column packed with pozzolan. At regular intervals, the differential pressure was measured using a manometer (Leol Keeler, France). The graphical representation of the equation below as a function of the variable  $\beta$  is a straight line with a slope of  $1/\psi^2$ .

Where:  $\psi$  represents the sphericity of the particle,  $\beta$  is related to the permeability (ease of flow) of the bed.

$$\frac{\Delta P}{H} = \frac{1}{\psi^2} * \beta = \frac{1}{\psi^2} * \frac{180 * \mu * v * (1 - \epsilon)^2}{d_p^2 \epsilon^3} \quad (3)$$

The specific surface area of the bed is determined by the expression:  $S_B = S_p(1 - \varepsilon)$  (4)

In which  $S_p$ , is the specific surface area of the particle and  $\varepsilon$  is the porosity of the bed; With :

$$S_p = \frac{6}{\psi d_p} \quad (5)$$

Where  $d_p$  is the diameter of the particle.

The density of a solid is the ratio of the aggregate's density to the density of water. If a quantity of aggregate is added to a container of water, the aggregate displaces a certain volume of water. The density is equal to the ratio of the mass of the aggregate to the mass of the displaced water.

$$D = \frac{(\text{mass of material})}{(\text{mass of displaced water})} \quad (6)$$

## 2.6. Hydrodynamics (flow regime) in the various filters

The experimental investigation of solute transport through a porous medium involves the injection of a tracer, or input function, into a packed column, followed by monitoring the system's response, known as the breakthrough curve (Deepak et al., 2013). In this study, a 1 M glucose solution was introduced into the column using a peristaltic pump (Gilson, France). After a defined flow period, the effluent was collected, and its refractive index was measured using an ATC refractometer. The measured values were then converted to solute concentration using a previously established calibration curve (Ref. GOD). All measurements were conducted at a controlled temperature of  $23 \pm 2$  °C. The breakthrough curve was generated by recording the glucose concentration at the outlet of the column as a function of the solution volume or elapsed time.

$$C/C_0 = f(V) \quad (7).$$

With  $C$  and  $C_0$  the concentrations at the outlet and inlet of the bed and  $V$  the volume of the solution.

## 2.7. Determination of retention

The Iwazaki Model (1937) is used to determine particle retention in the different beds (mixed and bilayer) because it takes into account particle accumulation in the flow phase. These equations are:

$$v \frac{\partial C_p}{\partial l} + (1 - \varepsilon_d) \frac{\partial \sigma}{\partial t} = 0 \quad (8)$$

$$\frac{\partial \sigma}{\partial t} = - \frac{v}{1 - \varepsilon_d} * \frac{\partial C_p}{\partial l} \quad \text{With} \quad - \frac{\partial C_p}{\partial l} = \lambda C \quad (9)$$

Where:  $v$  is the filtration rate;  $C_p$  is the particle concentration;  $l$  is the bed height;  $\sigma$  is the retention;  $t$  is the time;  $\lambda$  is the filtration efficiency; and  $\lambda_0$  is the efficiency at time zero.

## 3. Results and discussion

### 3.1. Bed characteristics

Table 1 indicates that the hydrodynamic properties of the mixed bed are superior to those of the bi-layer, pozzolan, and limestone beds, despite having identical particle density, sphericity, and specific surface area to the bi-layer configuration. The higher porosity of the mixed bed ( $67.24 \pm 0.3\%$ ) compared to the other media suggests a larger fluid-medium contact area, which promotes enhanced capture of suspended particles. Although the permeability of the mixed bed ( $5.73 \times 10^{-7} \pm 0.04$ ) is slightly higher than that of the bi-layer bed ( $3.51 \times 10^{-7} \pm 0.05$ ), both values remain within the same order of magnitude. Nevertheless, higher permeability facilitates improved filtration flow rates without inducing excessive pressure loss, which is a notable operational advantage. Furthermore, the increased specific surface area of the mixed bed ( $3334.22 \pm 6$ ) may contribute to more effective particle retention. Regarding

particle morphology, pozzolan and limestone exhibit relatively angular shapes due to their sphericity. However, pozzolan particles possess a significantly higher specific surface area ( $16,000 \pm 10$ ) compared to limestone particles ( $2,000 \pm 7$ ), which may account for their superior retention capacity.

**Table 1: Characteristics of the particle beds**

Characteristics	Bed Pozzolan	Bed Limestone	Bed Double	Bed Mixed
Density ( $\text{kg/m}^3$ )	$497 \pm 2.4$	$693 \pm 5.2$	$1189.58 \pm 5.03$	$1189.58 \pm 4.1$
Sphericity	$0.25 \pm 0.01$	$0.20 \pm 0.05$	$0.45 \pm 0.01$	$0.45 \pm 0.04$
Specific particle surface area ( $\text{m}^{-1}$ )	$16000 \pm 10$	$2000 \pm 7$	$8889 \pm 13$	$8889 \pm 11$
Bed porosity (%)	$49.70 \pm 0.5$	$40.00 \pm 0.3$	$62.49 \pm 0.3$	$67.24 \pm 0.3$
Specific surface area of the bed ( $\text{m}^1$ )	$9600 \pm 12$	$1006 \pm 9$	$2912 \pm 11$	$3334.22 \pm 6$
Bed permeability ( $\text{m}^2$ )	$5.45 \cdot 10^{-8} \pm 0.06$	$1.60 \cdot 10^{-8} \pm 0.08$	$3.51 \cdot 10^{-7} \pm 0.05$	$5.73 \cdot 10^{-7} \pm 0.04$
Reynolds number	$0.19 \pm 0.02$	$0.14 \pm 0.03$	$1.42 \pm 0.03$	$1.75 \pm 0.01$

### 3.2. Hydrodynamics of fixed two-layer and mixed limestone-pozzolan beds

Figure 4 illustrates the hydrodynamic behavior of both the two-layer and mixed filter beds. The non-Gaussian shape of the breakthrough curve suggests a laminar flow regime, which indicates the absence of preferential flow paths within the particle bed. As a result, axial diffusion appears to be the dominant transport mechanism within the medium. Under these conditions, the Reynolds number was calculated to be approximately 2,000. These findings align with those reported by Djehiche et al. (2015), who observed similar behavior using sand as the filtration medium. Furthermore, given that the ratio of the column diameter to the mean particle diameter exceeds 100, the use of the Kozeny–Carman equation is justified for describing flow through the bed.

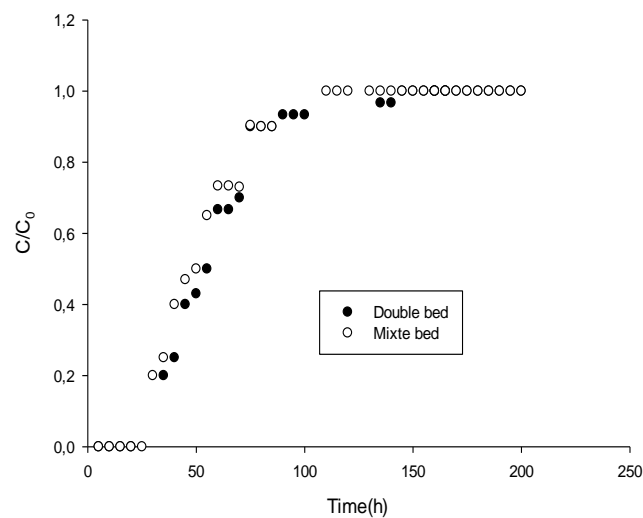


**Figure 4:** Breakthrough curve of the tracer (glucose) in the double and mixed bed pozzolan-limestone (H: 40 cm; T:  $23 \text{ }^\circ\text{C} \pm 2$ ; speed:  $9.8 \text{ cm}\cdot\text{min}^{-1}$ ,  $^\circ\text{Brix}$ :  $3 \pm 0.1$ )

### 3.3. Influence of the type of filtering material on abatement

Figure 5 illustrates that both curves exhibit a similar upward trend and share the same general shape. Three distinct phases can be identified. During the initial 120 minutes, both filters undergo a maturation phase characterized by a low turbidity removal efficiency—less than 30%. In this phase, particle removal rates increased by approximately 16% and 20% for the pozzolan and limestone beds, respectively. After 140 minutes, a plateau is observed in both cases, indicating that the turbidity reduction rate has reached a steady state. These findings are in agreement with previous studies by James (1985), Desjardins (1990), and Ives (1980).

The limited performance of the monolayer filters can be attributed to the intrinsic properties of the materials. Both porosity (49.7% for pozzolan and 40% for limestone) and specific surface area play a crucial role in particle capture. The limestone bed exhibits slightly higher turbidity removal, likely due to its coagulant effect, resulting from the presence of calcium ions that promote the formation of larger flocs, which are more easily retained in the filter media. Although pozzolan also demonstrates some particle retention, its effect remains minimal. This is consistent with findings by Ndi et al. (2008), who reported that pozzolan-based granular filters possess limited colloid retention capacity. Conversely, Villabona-Ortíz et al. (2022) showed that limestone filters can retain colloidal particles with an efficiency of over 20–30%.

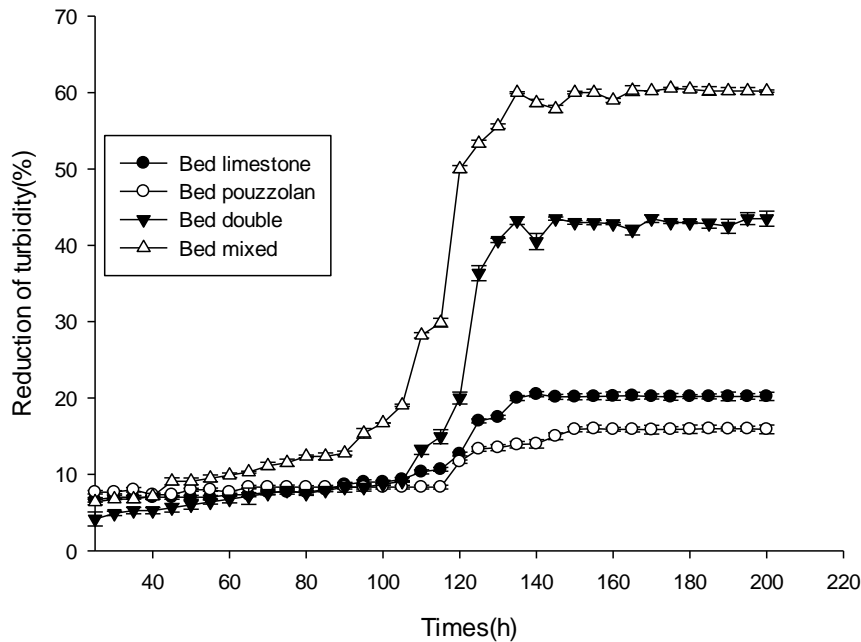


**Figure 5:** Variation in turbidity reduction in the filter material as a function of time (H:40 cm; T:23 ± 2°C; Turbidity: 30 NTU ± 1; pH: 6 ± 0.05, velocity: 9.8 cm.min<sup>-1</sup>).

During the first 50 minutes, both the bilayer and mixed filters display minimal turbidity reduction. Between 50 and 100 minutes, the mixed filter begins to outperform the bilayer filter, signaling the onset of its maturation phase. After 100 minutes, a clear distinction emerges, with the mixed filter achieving a turbidity reduction of approximately 61%, compared to 43% for the bilayer filter. This phase corresponds to the effective filtration stage. After 143 minutes, both curves level off, indicating stabilization.

This behavior can be explained by the structural characteristics of the mixed filter, which, despite being a combination of two materials, resembles a monolayer. This configuration facilitates the continuous dissolution of calcium ions throughout the bed, enhancing particle agglomeration. In contrast, the bilayer filter appears to be constrained by the presence of a distinct interface between the layers, limiting particle retention. These results are in line with observations by Zouboulis et al. (2007), who reported superior performance of bilayer filters compared

to monolayer configurations. However, the apparent contradiction is resolved by considering that the "monolayer" in this study consists of a mixture of two materials, enabling a synergistic coagulation–retention mechanism.

### 3.4. Influence of filter bed configuration on pH

Figure 6 displays a similar two-phase profile of pH evolution over time for all bed types. The first phase exhibits an exponential increase in pH, with the time required to reach the maximum pH varying between filter configurations. This is followed by a stationary phase, during which the pH remains constant. In the limestone bed, the material consists of more than 99% calcium carbonate ( $\text{CaCO}_3$ ), which is slightly soluble in water, and even more so under acidic conditions (initial suspension pH:  $6 \pm 0.05$ ). As dissolution proceeds, the pH increases until an equilibrium is established, stabilizing at approximately pH 8.5. This stabilization is attributed to the saturation of the solution with calcium and carbonate ions, which limits further dissolution of  $\text{CaCO}_3$ . The observed plateau corresponds to the buffering effect of the  $\text{HCO}_3^-/\text{CO}_3^{2-}$  equilibrium system.

In contrast, according to Ndi et al. (2016), pozzolan contains only 1.2%  $\text{CaO}$ , which explains the relatively modest pH increase in the pozzolan bed, despite its higher specific surface area compared to limestone, as shown in Table 1. Furthermore, Nguemtue et al. (2020) report that pozzolans do not engage in significant chemical interactions with acid ions that would notably affect pH, leading to the observed stabilization in the pozzolan bed.

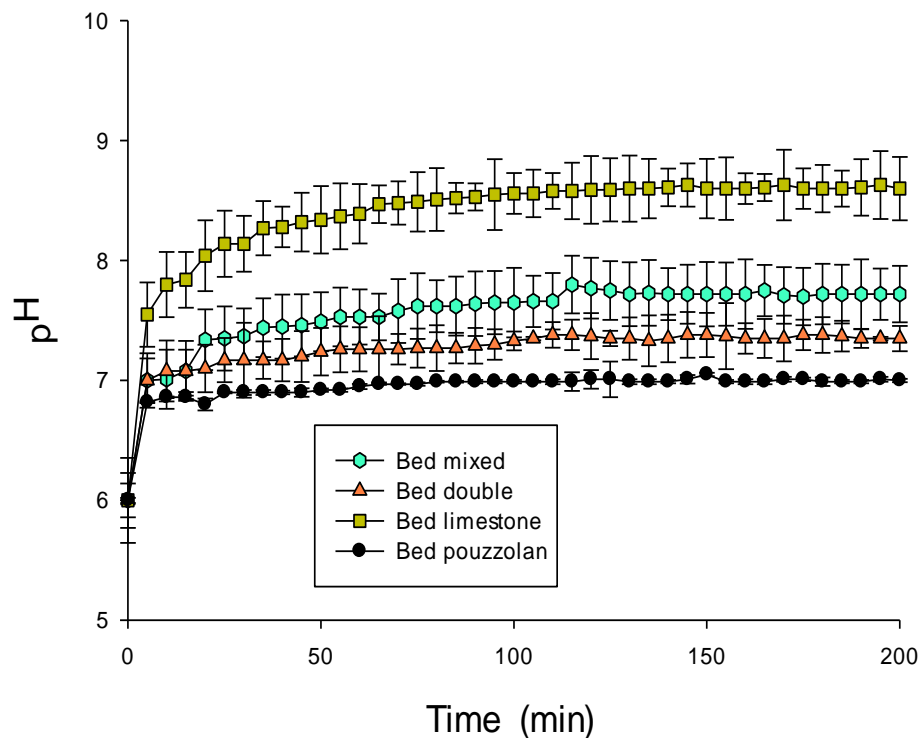


**Figure 6:** Variation of pH as a function of time in the configuration of filter beds on (H: 40cm; T:  $23 \pm 2$  °C; Turbidity:  $30 \pm 1$ , pH:  $6 \pm 0.05$ ; speed:  $9.8 \text{ cm}\cdot\text{min}^{-1}$ )

The specific surface area (reaction surface) of the bilayer bed is  $2911.99 \text{ m}^{-1}$ , whereas that of the mixed bed is  $3334.22 \text{ m}^{-1}$ . In the bilayer bed, pH increases due to the partial dissolution of limestone, which occurs as the suspension passes through the limestone layer before reaching the pozzolan layer. However, the contact time is relatively short, leading to a final pH stabilization around 7.5. In contrast, in the mixed bed, limestone and pozzolan particles are homogeneously distributed throughout the column, allowing more prolonged and uniform interactions between the suspension and the reactive materials. This configuration promotes a synergistic effect between the pozzolan and limestone, resulting in more effective and stable pH regulation.

### 3.5. Head loss in filter A beds

Figure 7 shows that both pressure drop curves are similar in shape and remain relatively stable over time. In the mixed bed, the initial pressure drop is around 600 Pa—corresponding to the baseline when distilled water is introduced—and quickly stabilizes near 775 Pa before slightly decreasing and settling at approximately 766 Pa. In the two-layer filter, the initial pressure drop is also 600 Pa but peaks at 1030 Pa within the first five minutes, then stabilizes. According to Mehryar et al. (2023), Overlay et al. (2002), and Bedrikovetsky et al. (2001), this early increase in head loss is due to the activation of filtering particles through wettability, which causes slight compaction of the bed, reducing porosity and increasing flow resistance. After this short activation period, the pressure drop stabilizes, indicating a steady flow velocity, as confirmed by Figure 4. The difference in pressure drop between the two beds is primarily attributed to their porosity levels, as shown in Table 1, with lower porosity resulting in higher head loss.

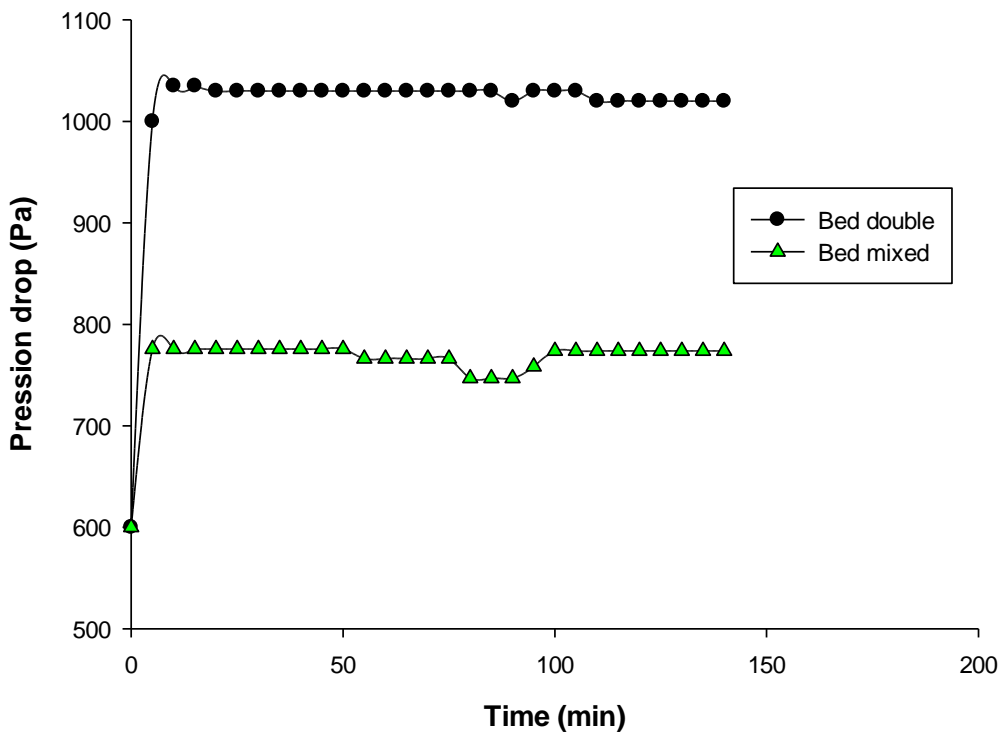


**Figure 7:** Variation in pressure drop as a function of time (H: 40 cm; T:  $23 \pm 2$  °C; Turbidity:  $30 \pm 1$  NTU; pH:  $6 \pm 0.05$ ; velocity:  $9.8 \text{ cm}\cdot\text{min}^{-1}$ ).

### Conclusion

The objective of this study was to identify the most effective filter configuration—monolayer, bilayer, or mixed—using pozzolan and/or limestone for the clarification of lateritic suspensions. Among all tested configurations, the mixed filter exhibited superior performance, achieving a turbidity removal efficiency of 61% and maintaining a stable pH of 7.5, in accordance with drinking water quality standards. Furthermore, the favorable hydrodynamic behavior and filtration efficiency of the mixed bed suggest its strong potential for application in similar water treatment contexts.

### Financial supports

No funds, grants or other financial support was received to conduct this study or to prepare the manuscript.

## Data Availability

The authors declare that the data supporting the findings of this study are available within the paper

## Competing interests

The authors declare that they have no known competing financial interests or personal relationships that could have appeared to influence the work reported in this paper.

## Acknowledgements.

The authors gratefully acknowledge the Chief of the Biochemical and Alimental Technologic Laboratory at the University of Ngaoundéré, as well as the respective heads of the Doctoral Training Unit in Engineering Sciences and the Doctoral School of Fundamental and Applied Sciences at the University of Douala. Special thanks are also extended to Mr. Fotsop Cyrille Ghislain of the Institute of Chemistry, Faculty of Process and Systems Engineering, Universitätplatz 2, 39106 Magdeburg, Germany, for his valuable assistance and availability in the characterization of biomasses.

## References

- [1] Abdou, K. D., Yayé, M., & Abdoulaye, A. (2024). Stratégies d'adaptation des populations à la précarité hydrique dans la ville de Zinder, Niger. *Canadian Journal of Development Studies*, 45(2). <https://doi.org/10.1080/02255189.2023.2285800>
- [2] Aguiza, A. E., Ombolo, A., Ngassoum, M. B., & Mbawala, A. (2014). Suivi de la qualité physico-chimique et bactériologique des eaux des cours d'eau de Ngaoundéré, au Cameroun. *Afrique Science*, 10(4), 135–145.
- [3] Badalians, G. G., Dehghanifard, E., Noori Sepehr, M., Torabian, A., Moalej, S., Dehnavi, A., Yari, A. R., & Asgari, A. R. (2012). Performance evaluation of different filter media in turbidity removal from water by application of modified qualitative indices. *Iranian Journal of Public Health*, 41(4), 87–93.
- [4] Basma, A. A., & Hussein, B. O. (2015, July). Evaluation of alum/lime coagulant for the removal of turbidity from Al-Ahdab Iraqi oilfields produced water. *Journal of Engineering*, 21(7), 145–153. <https://doi.org/10.31026/j.eng.2015.07.11> .
- [5] Bedrikovetsky, P., Marchesin, D., Shecaira, F., Souza, A. L., Milanez, P. V., & Rezende, E. (2001). Characterisation of deep bed filtration system from laboratory pressure drop measurements. *Journal of Petroleum Science and Engineering*, 32(2–4), 167–177. [https://doi.org/10.1016/S0920-4105\(01\)00159-0](https://doi.org/10.1016/S0920-4105(01)00159-0)
- [6] Besbes, S. (2020). *Performances du média Filtralite® appliqué à la filtration directe à la Ville de Montréal* [Master's thesis, Polytechnique Montréal]. PolyPublie. <https://publications.polymtl.ca/4150/>
- [7] Chegaing, S. P., Gingir, B., Nodem, S. F., Fadimatou, M. Y., Tepongning, N. R., Talom, B. T., & Gatsing, D. (2024). Water-related diseases in the Adamawa region, Cameroon: A prospective and retrospective case study and the susceptibility of isolated bacteria to common antibiotics. *Journal of Advances in Microbiology*, 21(7), 75–85. <https://doi.org/10.9734/JAMB/2021/v21i730370>
- [8] Deepak, S., Sharma, P. K., & Ojha, C. S. P. (2013). Experimental investigation of solute transport in stratified porous media. *ISH Journal of Hydraulic Engineering*, 19(3), 145–153. <https://doi.org/10.1080/09715010.2013.793930>
- [9] Djehiche, A., Gafsi, M., Canseco, V., Omari, A., & Bertin, H. (2015). Effet de la force ionique et hydrodynamique sur le dépôt de particules colloïdales dans un milieu poreux consolidé. *The Canadian Journal of Chemical Engineering*, 93, 781–787. <https://doi.org/10.1002/cjce.22151>

- [10] Ives, K. (1980). Deep bed filtration: Theory and practice. *Filtration and Separation*, 17(2), 157–168.
- [11] Iwasaki, T. (1937). Some notes on sand filtration. *Journal of the American Water Works Association*, 29, 1591–1602.
- [12] James, M. (1985). *Water treatment: Principles and design*. New York: Wiley and Sons.
- [13] Kameni, N. M., Ndi, K. S., Kofa, G. P., & Kayem, G. J. (2019). Coagulation and sedimentation of concentrated laterite suspensions: Comparison of hydrolyzing salts in presence of *Grewia* spp. biopolymer. *Journal of Chemistry*, 2019, Article ID 1431694. <https://doi.org/10.1155/2019/1431694>
- [14] Kepdieu, J. M., Tchanang, G., Njimou, J. R., Ekani, C. J., Njiomou Djangang, C., Maicaneanu, S. A., & Rosso, D. (2025). Mathematical modeling using full factorial design applied in the adsorption of dye Basic Blue 9 from synthetic aqueous solutions onto *Oryza sativa* husk-derived nano-silica-smectic clay composite. *Water, Air, & Soil Pollution*, 236, 49. <https://doi.org/10.1007/s11270-024-07676-3>
- [15] Legube, B. (2021). *Production d'eau potable* (2nd ed.). Dunod.
- [16] Lengaye, S.-C., Bomangayen, J. B., M'boliguipa, J., & Mouangue, R. M. (2019). Étude expérimentale et comparative de filtre composite en argile, charbon actif et filtre moderne à partir des analyses des quatre échantillons des eaux de Dang de la région de l'Adamaoua. *Journal of the Cameroon Academy of Sciences*, 15(2). <https://doi.org/10.4314/jcas.v15i2.2>
- [17] Mehryar, A. H., Serveh, K., Muhammad, S., & Pejman, T. (2023). Effect of wettability on two-phase flow through granular porous media: Fluid rupture and mechanics of the media. *Chemical Engineering Science*, 269, 118446. <https://doi.org/10.1016/j.ces.2023.118446>
- [18] Moye, E. K., Tiomo, D. E., & Otombaye, P. (2025). Unequal access to drinking water in the city of Doba (Chad): An urban political ecology perspective. *Eco Cities*, 6(1), 3001. <https://doi.org/10.54517/ec3001>
- [19] Ndi, K. S., Nsoe, M. J.-J. N., Kofa, G. P., Bessalla, P. E., Amba, V., & Kayem, J. G. (2016). Évaluation de la durée d'inoculation d'un biofiltre granulaire de pouzzolane à partir des souches indigènes de bactéries et de levures isolées d'effluent d'industrie de caoutchouc. *Revue des sciences de l'eau / Journal of Water Science*, 29(1), 27–34. <https://doi.org/10.7202/1035714a>
- [20] N Ndi, K. S., Mbundapong, N. L., Tatsadjieu, L., Ali, A., & Kayem, J. (2010). Retention of *E. coli* on natural pouzzolan beds. *Journal of Engineering and Applied Sciences*, 5(6), 430–434. <https://doi.org/10.3923/jeasci.2010.430.434>
- [21] Ndi, K., Dihang, D., Aimar, P., & Kayem, J. (2008). Retention of bentonite in granular natural pozzolan: Implications for water filtration. *Separation Science and Technology*, 43(7), 1621–1631. <https://doi.org/10.1080/01496390801974712>
- [22] Nguemtue, T. N., Kamga, R., Sieliechi, J. M., & Kayem, J. (2020). Evaluation of two white marbles for the correction of the aggressivity of fresh water of rivers. *Scientific African*, 10, e00601. <https://doi.org/10.1016/j.sciaf.2020.e00601>
- [23] Nguemtue, N. T., Ndiapa, F., Nsoe, M. J. J., Kofa, G., Kayem, J., Lartiges, B., Nguetnkam, J. P., Djieto, L. A. E., & Kamga, R. (2023). Typologie des calcaires du Cameroun pour la reminéralisation des eaux douces : Morphologie, minéralogie et géochimie. *Journal of Materials and Environmental Science*, 14(11), 1323–1335.
- [24] Overlay, P. P., Hapgood, J. D., Litster, S. R., & Biggs, T. H. (2002). Drop penetration into porous powder beds. *Journal of Colloid and Interface Science*, 253(2), 353–366. <https://doi.org/10.1006/jcis.2002.8527>

- [25] Raouf, A., Njeudjang, K., & Youmbi, J. G. T. (2025). Factors influencing groundwater development and mitigation strategies in Adamawa region, Cameroon: A critical review. *Sustainable Water Resources Management*, 11, Article 5. <https://doi.org/10.1007/s40899-024-01187-z>
- [26] Singh, V. (2024). Water resources. In *Textbook of environment and ecology* (Chapter 7). Springer, Singapore. [https://doi.org/10.1007/978-981-99-8846-4\\_7](https://doi.org/10.1007/978-981-99-8846-4_7)
- [27] Tangwa, B., Keubou, H., Nfor, E., & Ngakou, A. (2019). Antimicrobial resistance profile of bacteria isolated from boreholes and hand dug wells water in Ngaoundere Municipality of Adamawa Region in Cameroon. *Advances in Microbiology*, 9(7), 629–645. <https://doi.org/10.4236/aim.2019.97039>
- [29] Villabona-Ortíz, A., Tejada-Tovar, C., & López-Barbosa, D. (2022). Hydrodynamic evaluation of a filter bed of porous material from stratified sedimentary rocks for the removal of turbidity in surface waters. *South African Journal of Chemical Engineering*, 39, 97–105. <https://doi.org/10.1016/j.sajce.2021.10.002>
- [30] Wamba, A. G. N., Lima, E. C., Ndi, S. K., dos Reis, G. S., de Brum, I. A. S., Thue, P. S., ... & Dias, S. L. P. (2017). Synthesis of grafted natural pozzolan with 3-aminopropyltriethoxysilane: Preparation, characterization, and application for removal of Brilliant Green 1 and Reactive Black 5 from aqueous solutions. *Environmental Science and Pollution Research*, 24, 21807–21820. <https://doi.org/10.1007/s11356-017-9825-4>
- [31] Zouboulis, A., Traskas, G., & Samaras, P. (2007). Comparison of single and dual media filtration in a full-scale drinking water treatment plant. *Desalination*, 213, 334–342. <https://doi.org/10.1016/j.desal.2006.02.102>